Heliyon 10 (2024) e29291

Contents lists available at ScienceDirect

Heliyon

journal homepage: www.cell.com/heliyon

Research article

Melatonin inhibits tongue squamous cell carcinoma: Interplay of ER stress-induced apoptosis and autophagy with cell migration

Huimin Liu [a,b,1], Ye Zheng [c,1], Shaoning Kan [a], Ming Hao [a], Huan Jiang [d], Shuangji Li [a], Rong Li [e], Yinyu Wang [f], Dongxu Wang [e,*], Weiwei Liu [a,**]

[a] Department of Oral and Maxillofacial Surgery, Hospital of Stomatology, Jilin University, Changchun, 130021, China
[b] Department of Stomatology, Shunyi District Hospital, NO.3 Guangming South Street, Shunyi District, Beijing 101300, China
[c] Department of Anesthesiology, Hospital of Stomatology, Jilin University, Changchun, 130021, China
[d] Department of Orthodontics, Hospital of Stomatology, Jilin University, Changchun, 130021, China
[e] Laboratory Animal Center, College of Animal Science, Jilin University, Changchun, China
[f] Stomatology Hospital, Baicheng Medical College, Baicheng, 130300, China

ARTICLE INFO

Keywords:
Tongue squamous cell carcinoma
Endoplasmic reticulum stress
Apoptosis
Autophagy
Cell migration

ABSTRACT

Tongue squamous cell carcinoma (TSCC) occupies a high proportion of oral squamous cell carcinoma. TSCC features high lymph node metastasis rates and chemotherapy resistance with a poor prognosis. Therefore, an effective therapy strategy is needed to improve patient prognosis. Melatonin (MT) is a natural indole compound shown to have anti-tumor effects in several cancers. This study focused on the role and mechanism of MT in TSCC cells. The results of the study suggest that MT could inhibit cell proliferation in CRL-1623 cells. Western blot analysis showed the down-regulate of cyclin B1 and the up-regulate P21 protein by MT. MT was also shown to down-regulate the expression of Zeb1, Wnt5A/B, and β-catenin protein and up-regulate E-cadherin to inhibit the migration of CRL-1623 cells. MT also promoted the expression of ATF4, ATF6, Bip, BAP31 and CHOP in CRL-1623 cells leading to endoplasmic reticulum stress, and induced autophagy and apoptosis in CRL-1623 cells. Western blots showed that MT could promote the expression of Bax, LC3, and Beclin1 proteins and inhibit the expression of p62. We screened differentially expressed long non-coding RNAs (lncRNAs) in MT-treated cells and found that the expression of *MALAT1* and *H19* decreased. Moreover, MT inhibited tumor growth in nude mice inoculated with CRL-1623 cells. These results suggest that MT could induce autophagy, promote apoptosis, and provide a potential natural compound for the treatment of TSCC.

1. Introduction

Head and neck cancers, including oral cancer, are some of the most common malignancies worldwide [1]. Tongue squamous cell carcinoma (TSCC) is the most prevalent type of oral malignancy [2]. Although modern medical therapy has made considerable

* Corresponding author. Laboratory Animal Center, College of Animal Science, Jilin University, Heping Campus, 1977 Xinzhu Road, Green Park, Changchun, Jilin Province, 130000, China.
** Corresponding author. Department of Oral and Maxillofacial Surgery, Hospital of stomatology, Jilin University, 1500 Qinghua Road, Changchun, Jilin Province, 130021, China.
E-mail addresses: wang_dong_xu@jlu.edu.cn (D. Wang), liuweiw@jlu.edu.cn (W. Liu).
[1] The authors Contributed equally to this work.

https://doi.org/10.1016/j.heliyon.2024.e29291
Received 24 November 2023; Received in revised form 1 April 2024; Accepted 4 April 2024
Available online 9 April 2024

progress, the effects of therapy for TSCC remain unsatisfactory, and the five-year survival rate of patients is low [3]. The therapeutic strategies for TSCC include surgical resection combined with radiotherapy and chemotherapy [4]. However, this therapeutic strategy reduces the patient's quality of life [5], and chemotherapy resistance is a factor hindering the treatment of TSCC(6). Therefore, exploring new therapeutic drugs is necessary. Natural compounds are promising anti-cancer drugs, and several natural molecular compounds, such as curcumin [6], cucurbitacin B (CuB) [3], and melatonin (MT), have been used to treat cancer [7]. This study is dedicated to elucidating the therapeutic potential of MT in TSCC.

MT is a natural indole compound that exists widely in animals and is mainly secreted by the pineal gland [8]. MT is also found in many plants [9]. The most well-known function of MT is in regulating circadian rhythms [10]. However, MT also has immune regulation [11], anti-inflammatory [12], anti-oxidant [13], vascular regulation [14], and anti-cancer activities [7]. Studies have shown a close relationship between MT and cancer and the anti-cancer effects of MT on cancer cells [15,16]. MT inhibited the proliferation and metastasis of prostate cancer and, thus, tumor progression [17]. MT was shown to promote apoptosis and activate the p53 gene to inhibit breast cancer [15]. MT induced apoptosis, inhibited oxidative stress in cervical cancer cells and enhanced the effect of chemotherapy in the treatment of cervical cancer [18]. Besides promoting apoptosis in cancer cells, MT was also shown to promote autophagic cell death in cancer cells [19]. Previous reports suggested that MT could induce cellular autophagy and promote colorectal cancer cell death [19]. These findings suggest that MT could inhibit tumor growth and induce tumor cell death through multiple mechanisms. This study focuses on elucidating the mechanisms through which MT induces cell death in TSCC, contributing valuable insights into its potential therapeutic applications for TSCC treatment.

In Addition, endoplasmic reticulum stress also induces cell death [20]. The endoplasmic reticulum (ER) plays a crucial role in protein synthesis and maturation, as well as a calcium reservoir for maintaining intracellular calcium homeostasis [21]. When the function of the ER is impaired due to various factors, the ER undergoes a stress response, which is manifested by the accumulation of large amounts of unfolded and misfolded proteins within the ER compartments as well as disturbances in intracellular calcium homeostasis [22,23]. The ER performs its normal role is maintained by the UPR through three signaling pathways, including PERK, IRE1, and ATF6(24). These signaling pathways can maintain ER protein stability by dynamically adjusting ER folding capacity and sustain cellular functions under endoplasmic reticulum stress [24]. However, prolonged UPR activation leads to cell death. Whether MT can lead to cell death by inducing endoplasmic reticulum stress is also one of the concerns of this study.

Previous research has demonstrated that a multitude of long non-coding RNAs (LncRNAs) are abnormally expressed in TSCC, playing a pivotal role in the regulatory mechanisms of tumor progression. Different LncRNAs exert distinct roles, influencing the advancement of TSCC in various aspects such as cell migration, autophagy, apoptosis, proliferation, invasion, and cellular drug resistance, through diverse signaling pathways [3,25,26,27]. A study suggested that knocking out *LncRNA CASC9* in TSCC cells SCC15 and CAL27 significantly promotes autophagy and apoptosis while inhibiting proliferation [28,29]. Furthermore, the application of certain drugs can target these LncRNAs to curb the growth of TSCC(3). A recent study found that ginsenoside Rd can inhibit the expression of *LncRNA H19*, thereby impeding the progression of TSCC(29). In this study, we will also investigate whether MT can affect the progression of TSCC through the modulation of LncRNAs.

2. Materials and methods

2.1. Cell culture and treatments

Human TSCC cell lines CAL-27 and CRL-1623 (SCC-15) were cultured in Dulbecco's modified Eagle's medium (DMEM; Gibco, Gaithersburg, MD, USA) and SCC-9 in DMEM/F12 (DMEM/F12; Gibco). Fetal bovine serum (FBS, 10 %) (Gibco, Gaithersburg, MD, USA) and penicillin/streptomycin (1 %) (Meilunbio, Dalian, China) were used in the medium for cell culture. The cell culture conditions were 37 °C in 5 % CO_2. MT was procured from Sigma-Aldrich (Shanghai, China). During the experiments, MT was dissolved in a mother liquor concentration of 5 mol/L DMSO and diluted to the desired concentration with cell culture medium so that the maximum concentration of the drug was 5 mmol/L (maximum DMSO concentration was 1 ‰). In order to the validation of melatonin's effects, rapamycin (Alfa Aesar, Ward Hill, MA, USA) was introduced into the experimental conditions to assist in confirming the impact of melatonin on CRL-1623 cells. Rapamycin, dissolved in ethanol, was prepared as a stock solution with a concentration of 1 mmol/L and stored at −20 °C. During the experimental procedures, rapamycin was diluted with cell culture medium to the desired concentration for the treatment of CRL-1623 cells, ensuring that the maximum drug concentration in the experiments was 1000 nmol/L (with the ethanol concentration not exceeding 1 ‰).

2.2. Cell proliferation analysis

The proliferation of cells was analyzed by the Cell Counting Kit-8 (CCK-8) assay (Dojindo, Kumamoto, Japan). CAL-27, CRL-1623, and SCC-9 cells were seeded in 96-well plates (4×10^3) and treated with different concentrations of MT (0, 0.5, 1, 2.5, and 5 mmol/L). Then 10 μL of CCK-8 solution was added to each well and incubated for 2 h at 37 °C in 5 % CO_2. Cell viability was determined by absorbance (optical density) at 450 nm. The data were analyzed using GraphPad software (San Diego, California, USA) to determine the effect of MT on the proliferation of TSCC cells.

2.3. Cell cycle analysis

After CRL-1623 cells (1×10^5) were seeded into six-well plates and treated with MT (0, 0.5, 1, and 2.5 mmol/L) for 24 h, the cells

were collected using 0.1 % trypsin and washed twice with precooled phosphate buffer solution (PBS). Then, 70 % ethanol was added, and the cells were fixed at −20 °C overnight. Afterward, they were washed twice with pre-chilled PBS. After 15 min, the cells were dyed with propidium iodide (PI)/RNase staining buffer (San Jose, CA, USA) in the dark. The cell samples were analyzed by flow cytometry, and ModFit LT software was used to analyze the data.

2.4. Wound healing assay

The wound healing assay was performed to determine the migratory ability of the cells. CRL-1623 cells (5×10^5) were seeded into six-well plates and treated with MT (0, 0.5, 1, and 2.5 mmol/L) for 24 h. The scratched area of cell migration was observed at 0, 24 and 48 h, which was measured using ImageJ software to analyze the effect of MT on cell migration. All experiments were performed in triplicate.

2.5. Transwell assay

The Transwell assay was used to determine cell migration behavior. CRL-1623 cells were treated with MT (0, 0.5, 1, and 2.5 mmol/L) for 24 h, and 1×10^4 cells were added to the Transwell kit. Following this, 0.5 mL of medium containing 10 % FBS was added to the floor of the chamber. The cells were cultured for 24 h, and the bottom cells were fixed with paraformaldehyde (4 %) and dyed with crystal violet dye (0.1 %) (Solarbio, Beijing, China). Stained cells were observed using an inverted microscope.

2.6. Soft agar assay

CRL-1623 cells were treated with MT (0, 0.5, 1, and 2.5 mmol/L) for 24 h, and 0.5 % of the basal agar solution preheated to 37 °C was added to the six-well plates and solidified at 4 °C for 2 h. Pre-treated CRL-1623 cells (1×10^3), 0.35 % agar solution at 37 °C, and DMEM were added to the solidified basal agar. After the upper agar solution was solidified, it was cultured at 37 °C in 5 % CO_2 for 21 days. After 21 days, the cells were fixed with paraformaldehyde (4 %) and dyed with crystal violet dye (0.1 %). The stained cells were counted using an inverted microscope and ImageJ software.

2.7. Cell apoptosis analysis

CRL-1623 cells were treated with MT at (0, 0.5, 1, and 2.5 mmol/L) for 24 h and washed twice with PBS. The cells were collected and incubated according to the instructions of the AnnexinV-FITC/PI kit (Beyotime, Shanghai, China, Cat No. C1062L). Flow cytometry (CytoFLEX, Beckman Coulter biotechnology (Suzhou)) was used for cell fluorescence analysis.

2.8. Real-time quantitative PCR

CRL-1623 cells were treated with MT at (0, 0.5, 1, and 2.5 mmol/L) for 24 h. The TRIzol method was used to extract total RNA. cDNA was synthesized using the BioRT cDNA (Bioer Technology, Hangzhou, China) first-strand synthesis kit according to the manufacturer's instructions. The BioEasy SYBR Green I Real-time PCR kit (Beijing Tiangen) was used for quantitative PCR (qPCR). The qPCR experimental conditions were 95 °C for 3 min, then denaturation at 95 °C for 10 s and annealing at 60 °C for 15 s, followed by an extension at 72 °C for 30 s. Thus, there was a total of 40 denaturation cycles. GAPDH was used as the internal control. The primer sequences used for RT-qPCR are in Table S1. The mRNA expression of related genes was detected using the $2^{-\Delta\Delta CT}$method.

2.9. Western blots

CRL-1623 cells were treated with MT (0, 0.5, 1, 2.5 mmol/L) for 24 h, extracted with Beyotime protein extraction buffer, and quantitatively analyzed using the BCA protein analysis kit (Dalian Meilun, China). Then, 10 % sodium dodecyl sulfate-polyacrylamide gel electrophoresis was applied to separate the proteins, which were transferred to a polyvinylidene membrane. The membranes were then sealed with skim milk (5 %) powder and washed with TBST (Tris buffered salt solution with 0.1 % Tween-20). The membranes were incubated overnight with primary antibodies, including anti-cyclin B1 (ab32053, Abcam, Cambridge, MA, USA), anti-P21 (ab109520, Abcam), anti-β-actin (ab8226, Abcam), anti-Zeb1 (ab203829, Abcam), anti-c-myc (ab32072, Abcam), anti-β-catenin (ab32572, Abcam), anti-Wnt5A/B (55184-1-AP, Proteintech, Wuhan, China), anti-LC3 (ab62721, Abcam), anti-BAP31 (ab109304, Abcam), anti-Beclin1 (ab302669, Abcam), anti-BiP (ab21685, Abcam), anti-P62 (ab207305, Abcam), anti-p-c-myc (28915-1-AP, Proteintech), anti-E-cadherin (60335-1-Ig, Proteintech), anti-Bax (50599-2-Ig, Proteintech), anti-Bcl-2 (26593-1-AP, Proteintech), anti-IRE1α (27528-1-AP, Proteintech), anti-CHOP (15204-1-AP, Proteintech) and anti-GAPDH (MB9231, Bioworld, Beijing, China), then incubated for 2 h with affinity-purified goat IgG (Boster, Guangzhou, China) coupled with horseradish peroxidase (HRP), and finally, developed with ECL SuperSignal (Pierce, Rockford, IL, USA). Grayscale analysis of the protein bands was performed using ImageJ.

2.10. Staining of autophagic structures

DALGreen and DAPRed (Dojindo Molecular Technologies, Kumamoto, Japan) were used according to the supplier's protocol as

described below. The CRL-1623 cells were preincubated in a culture medium containing 1 μM DALGreen and 0.1 μM DAPRed for 30 min. After washing out the staining medium, the cells were treated with various concentrations of MT (0, 0.5, 1, and 2.5 mmol/L) for 48 h. Subsequently, fluorescence images were captured using a fluorescence microscope under identical conditions (same laser power and detector gains). The method was adapted from previously published research and has been appropriately cited in our study [30].

2.11. Animals and animal care

Ten 8-week-old nude mice (Control and experimental groups: three females, two males, about 20–25 g) were supplied by the Experimental Animal Center of Jilin University (No. SY202109003). The nude mice were grouped in laboratory cages and raised in specific-pathogen-free living conditions at 24 °C, relative humidity of 50–60 %, and 12 h light and dark cycles. The nude mice were provided with national standard rodent food and water. All of the nude mice were in good health and uninfected throughout the experiment. All surgeries were performed under germ-free conditions. Each nude mice were injected subcutaneously with CRL-1623 cells (8×10^6/200 μL) on the left side of the axilla. The general condition and tumor growth of the nude mice were observed once a day. After 10 days, the general condition of the nude mice was observed to be good, no death occurred, and the tumor volume was between 60 and 100 mm^3, not more than 150 mm^3. The nude mice did not show serious weight loss, no voluntary diet, infection, systemic organ failure, or tumor rupture. If the above conditions occurred, euthanasia should be performed promptly. Under general anesthesia (0.41 ml/min at 4 L/min Fresh gas flow), MT was injected intraperitoneally every two days, and melatonin was administered 1 h before the rise in endogenous melatonin levels at night (1 h before the room lighting was switched off), when tissues are most sensitive to the hormone [31]. In the experimental group, mice were intraperitoneally injected with a melatonin solution prepared in DMSO, which was originally concentrated 20 times and diluted to 75 mg/kg with saline before use. In the control group, mice were injected intraperitoneally with the same solution without melatonin. The nude mice were observed daily for systemic conditions, with no abnormalities noted. After 9 days no dead nude mice were found, the nude mice were placed in a small animal anesthesia chamber and given isoflurane for general anesthesia (0.41 ml/min at 4 L/min Fresh gas flow). The nude mice were anesthetized and dislocated at the cervical spine and executed. It was confirmed that the nude mice had no respiration, pulse, no heartbeat for more than 5 min by touching the heart part of the chest, the corneal reflex disappeared, the pupils were dilated, and the nerve reflex disappeared. After confirming the death of the nude mice, the nude mice were dissected and tumor data were recorded. The tumor volume was calculated based on the recorded length (L) and width (W) of the tumor ($L \times W^2/2$) [3]. Length represents the longest diameter of the tumor, while Width represents the perpendicular diameter of the tumor. The tumor volume and weight were then analyzed. The bodies were packed and sealed in special bags, and then placed in the designated freezers in the laboratory animal center for centralized frozen storage.

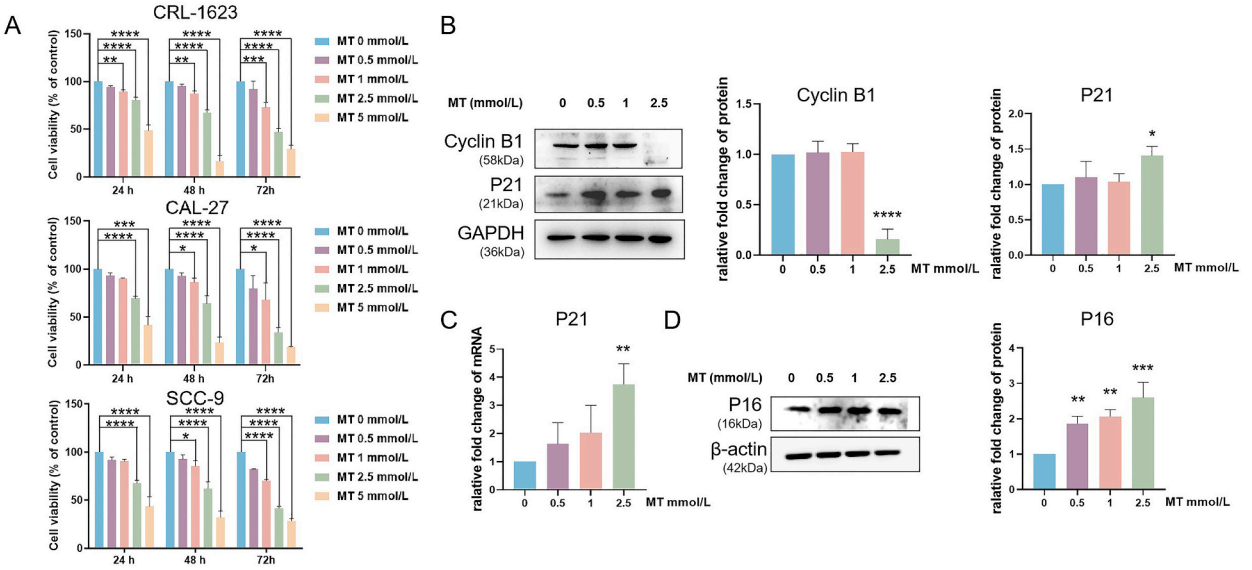

Fig. 1. (A) Effect of MT on cell proliferation. CRL-1623, CAL-27 and SCC9 cells were treated with different concentrations of MT and cell viability was assayed at different time points using CCK-8 assay. The results showed that MT had a dose-dependent inhibitory effect on the growth of the three TSCC cells. (B) CRL-1623 cells were treated with different concentrations of MT and analyzed by Western blot to assess the expression of Cyclin B1 and P21 protein. The bar graph shows the results of quantitative Western blot analysis. Non-adjusted images for Western blot are included as Supplementary Material. (C) CRL-1623 cells were treated with different concentrations of MT and RT-qPCR analysis was performed to assess P21 mRNA levels. (D) CRL-1623 cells were treated with different concentrations of MT and analyzed by Western blot to assess the expression of P16 protein, and the bar graph shows the results of quantitative Western blotting analysis. Non-adjusted images for Western blot are included as Supplementary Material. *P < 0.05, **P < 0.01, ***P < 0.001, ****P < 0.0001 vs. 0 mmol/L.

2.12. Statistical analysis

Differences in data across experimental groups were assessed using the One-way ANOVA. Unpaired Student's t-test was used to analyze the tumor volume and weight of mice. Statistical analyses were performed using GraphPad Prism software (GraphPad Software, Inc). *P < 0.05, **P < 0.01, ***P < 0.001, ****P < 0.0001 were considered to be statistically significant.

3. Results

3.1. MT suppresses the proliferation of TSCC cells

The CCK-8 assay was used to analyze the effect of MT on the proliferation of TSCC cells. Three types of TSCC cells (CRL-1623, CAL-27, and SCC-9) were treated with MT (0, 0.5, 1, 2.5, and 5 mmol/L) for 0, 24, 48, and 72 h. The results shown in Fig. 1A demonstrate that 2.5 mmol/L MT was effective in inhibiting cell proliferation at 24 h. MT caused great toxicity to CAL-27 and SCC-9 cells at 24 h, so CRL-1623 cells were selected for subsequent experiments. An MT concentration of 5 mmol/L was not chosen for subsequent experiments due to toxicity.

Cell proliferation is closely related to cell cycles [32]. Cell cycle arrest can result in the prolongation of the cell growth cycle and the slowing of cell proliferation [33]. CRL-1623 cells were treated with MT (0, 0.5, 1, and 2.5 mmol/L), and the protein expression levels of cyclin B1 were analyzed to investigate the effect of MT on cell cycle distribution in CRL-1623 cells. As shown in Fig. 1B, 2.5 mmol/L MT substantially downregulated cyclin B1 protein. Next, the expression of P21 protein was analyzed in CRL-1623 cells treated with MT. Western blots and real-time qPCR (RT-qPCR) analysis demonstrated that 2.5 mmol/L MT could up-regulate P21 protein. Furthermore, MT significantly promoted the expression level of P16 protein. These results indicate that MT can inhibit proliferation by blocking the cell cycle (Fig. 1B, C, D and S1).

3.2. MT suppresses the migration of CRL-1623 cells

The metastasis rate of TSCC is high, so the role of MT in TSCC migration was investigated [34]. Transwell and wound healing assays were used to determine changes in CRL-1623 cells migration after exposure to MT. CRL-1623 cells were treated with MT (0, 0.5, 1, and 2.5 mmol/L) for 24 h to determine changes in cell migration. The results in Fig. 2A and B shows that 2.5 mmol/L MT substantially inhibited the migration of CRL-1623 cells. In the wound healing assay, CRL-1623 cells were treated with MT (0, 0.5, 1, and 2.5 mmol/L) for 24 h, and the migratory ability of CRL-1623 cells was analyzed at 0, 24, and 48 h. As shown in Fig. 2C–D and S2, at 48 h, 2.5 mmol/L MT effectively inhibited the migratory ability of CRL-1623 cells.

Some genes related to cell migration (Zeb1, Wnt5A/B, β-catenin, c-myc, p-c-myc, and E-cadherin) were analyzed to further explore the mechanism of action of MT on the migration of CRL-1623 cells. The results in Fig. 3A show that MT could promote the expression of E-cadherin protein. Zeb1, Wnt5A/B, and β-catenin decreased substantially after treatment with 2.5 mmol/L MT (Fig. 3B–C, E). c-Myc and p-c-myc, the target genes of Wnt/β-catenin signal transduction, also decreased (Fig. 3D and E). Furtherly, we assayed the

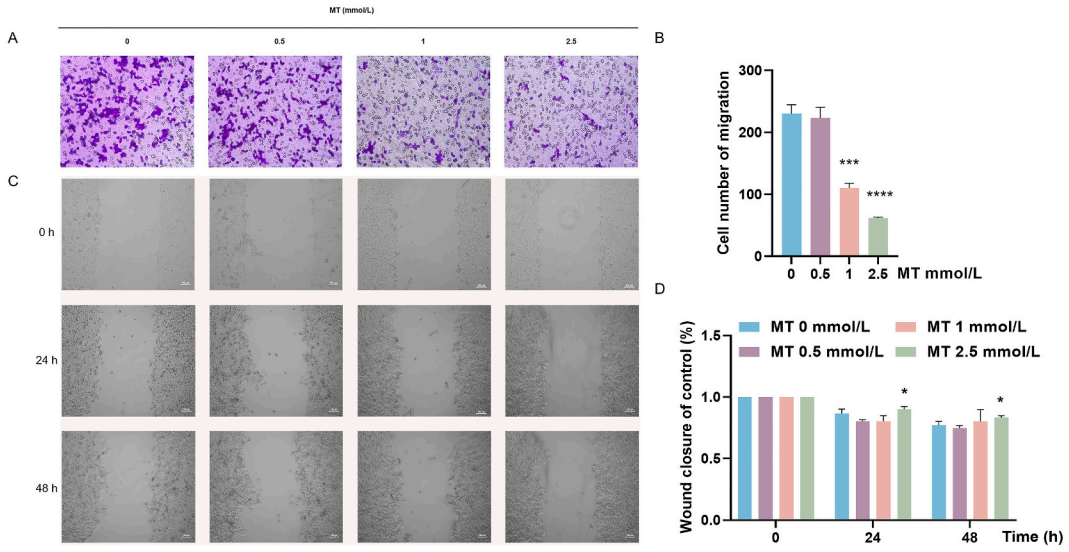

Fig. 2. (A–D) The effect of MT on cell migration. (A–B) CRL-1623 cells were treated with different concentrations of MT and then analyzed by Transwell assay. The bar graph shows the number of migrated cells. (C–D) Wound healing assay was performed after treatment of CRL-1623 cells with different concentrations of MT; the bar graph is quantitative analysis of wound healing area. *P < 0.05, ***P < 0.001, ****P < 0.0001 vs. 0 mmol/L.

expression of MMP9 protein and found that MT had no effect on MMP9 protein (Fig. S3). These results suggest that 2.5 mmol/L inhibited the migration of CRL-1623 cells.

3.3. MT induces the death of CRL-1623 cells

This study analyzed changes in the apoptosis of CRL-1623 cells after MT treatment. As shown in Fig. 4A and B, MT substantially induced the apoptosis of CRL-1623 cells in a dose-dependent manner. RT-qPCR and Western blot analyses were performed to investigate the expression pattern of apoptosis-related genes to further investigate the mechanism of action of MT on the apoptosis of CRL-1623 cells. The results in Fig. 4C–H shows that treatment with different concentrations of MT (0, 0.5, 1, and 2.5 mmol/L), increased HRK, TNFRSF10A, and TNFRSF10B, and the Bax/Bcl2 protein ratio was also up-regulated. This indicates that MT could induce apoptosis in CRL-1623 cells.

As MT may act similarly to the mTOR inhibitor rapamycin, we first verified the effect of rapamycin on CRL-1623 cells. CRL-1623 cells were processed with rapamycin at different concentrations (0, 50, 100, 200, 500, 1000 nmol/L) of rapamycin for 24 h, and changes in Beclin1 and LC3 proteins in the cells were analyzed. The results suggested that rapamycin promoted the expression of Beclin1 and LC3, which indicated that rapamycin might induce cellular autophagy (Fig. 5A and B). BAP31 and Bip were also increased, which suggested that rapamycin might cause endoplasmic reticulum (ER) stress (Fig. 5C and D). Subsequently, to determine whether MT induced autophagy in CRL-1623 cells, we further analyzed the expression of autophagy-related genes. As shown in Fig. 5E–I, the expression of autophagy-related genes LC3 and Beclin1 were up-regulated after MT treatment (0, 0.5, 1, and 2.5 mmol/L), whereas the protein level of p62 was decreased, indicating that MT could induce autophagy and lead to CRL-1623 cell death. To further verify whether MT induced autophagy, we detected the occurrence of autophagic flux by two novel probes DAL Green and DAPRed (Fig. S4). As shown in Fig. S4, CRL-1623 cells treated with different concentrations MT were co-cultured with DALGreen and DAPRed probes, respectively, and subsequently an increase in the signal intensity of DALGreen and DAPRed was observed under fluorescence microscope with the increase of MT concentration, which suggests that MT effectively promotes autophagic flux in CRL-1623 cells. The above results suggest that MT could induce apoptosis and autophagy in CRL-1623 cells, leading to cell death. As rapamycin induced ER stress, we further analyzed whether MT induced ER stress.

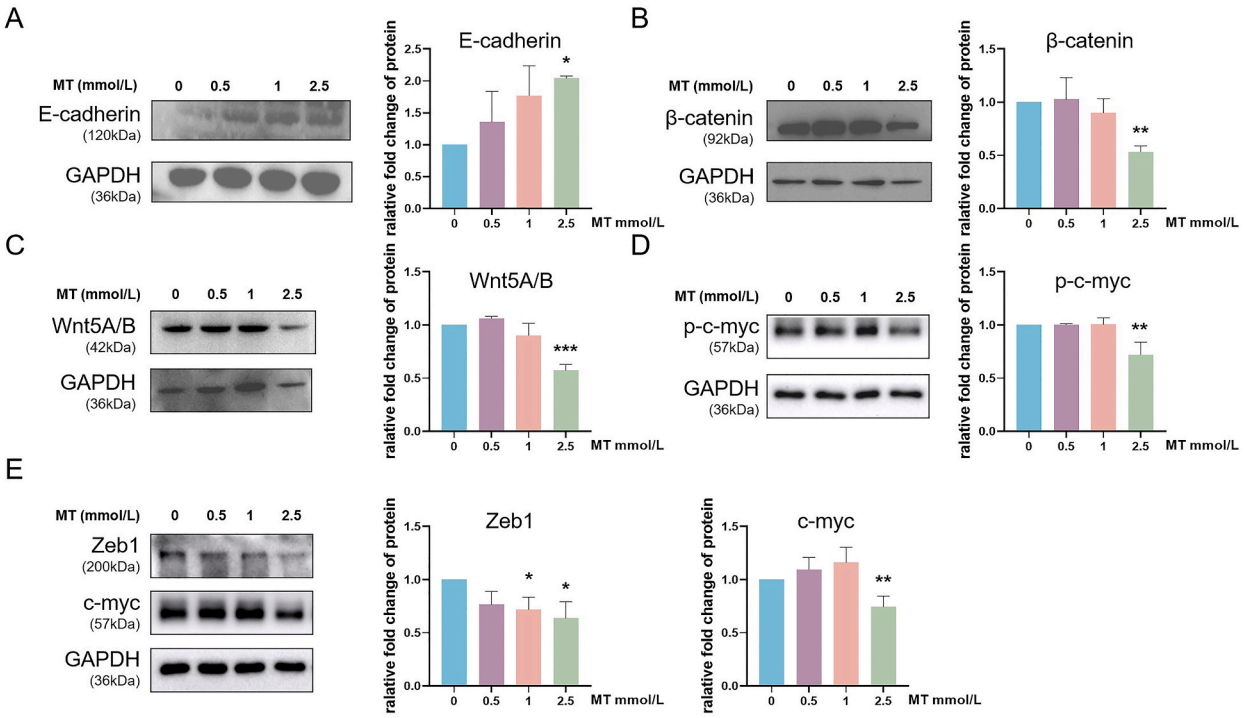

Fig. 3. (A) Western Blot was performed to analyze the expression of E-cadherin protein after treatment of CRL-1623 cells with different concentrations of MT; the bar graph shows the quantitative analysis of E-cadherin protein. Non-adjusted images for Western blot are included as Supplementary Material. (B–E) Western Blot analysis of the expression of cell migration-related proteins after treatment of CRL-1623 cells with different concentrations of MT, and the bar graphs show the quantitative analysis of these proteins. Non-adjusted images for Western blot are included as Supplementary Material. *P < 0.05, **P < 0.01, ***P < 0.001 vs. 0 mmol/L.

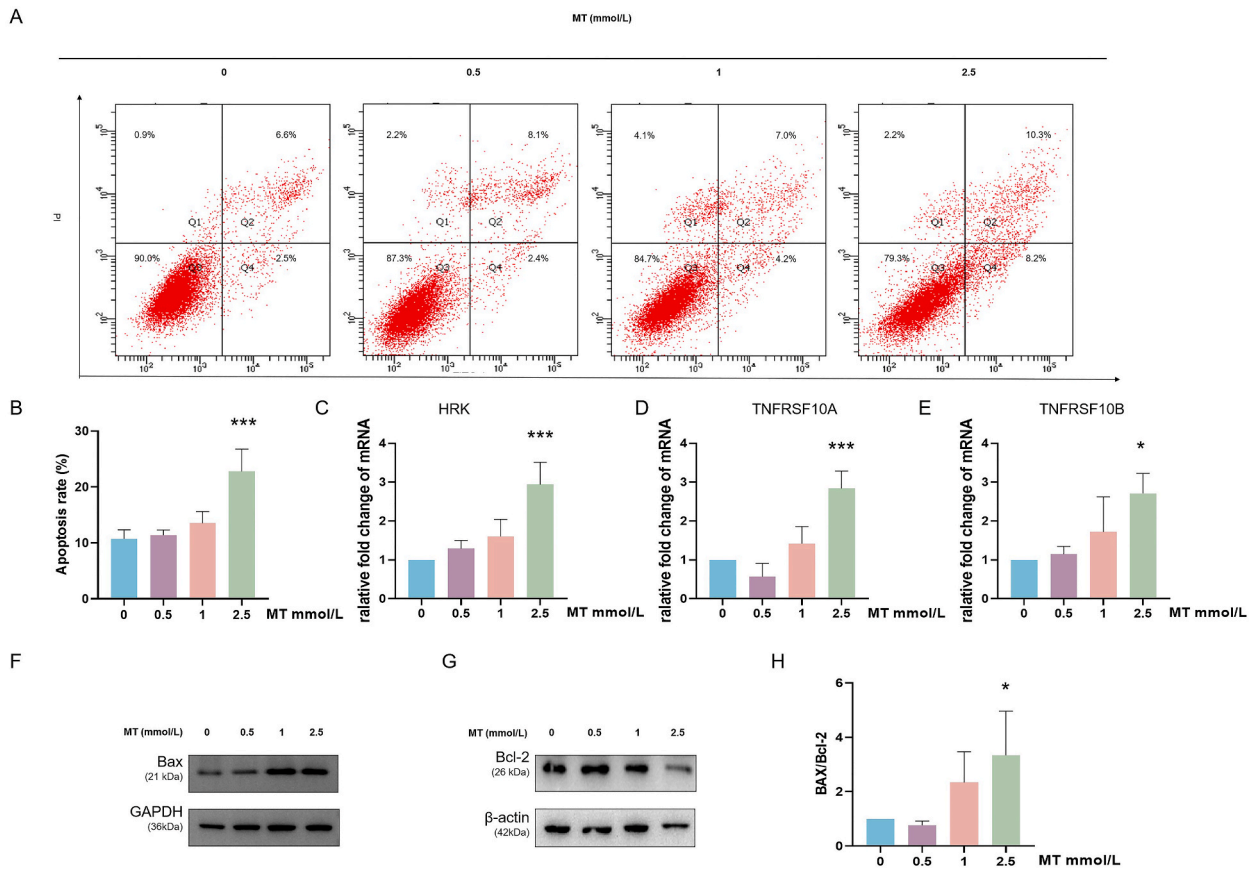

Fig. 4. (A) Effect of MT on apoptosis. The effect of MT on CRL-1623 cell apoptosis was analyzed by flow cytometry after treating CRL-1623 cells with different concentrations of MT. (B) Apoptosis rate of CRL-1623 cells represented in a bar graph. (C–E) RT-qPCR experiments were conducted to quantify the mRNA expression levels of HRK, TNFRSF10A, and TNFRSF10B in CRL-1623 cells following treatment with different concentrations of MT. (F–H) Western Blot analysis was performed to evaluate the expression levels of Bax and Bcl-2 proteins in CRL-1623 cells treated with varying concentrations of MT. The bar graph depicts the quantitative analysis of the Bax/Bcl-2 protein ratio. Non-adjusted images for Western blot are included as Supplementary Material. *P < 0.05, ***P < 0.001 vs. 0 mmol/L.

3.4. MT induces endoplasmic reticulum stress in TSCC cells

ER stress can induce cell death [35]. As previous studies showed that MT could induce the death of TSCC cells, we analyzed whether it could induce ER stress. ATF4, ATF6, Bip, BAP31, and CHOP were analyzed to determine whether MT could induce ER stress in CRL-1623 cells (Fig. 6A–B, D-E). Genes related to ER stress were increased after MT treatment (Fig. 6A–B, D-E). We also found that the IRE1-α pathway, associated with ER stress, was activated (Fig. 6C). The results showed that MT might interfere with the homeostasis of cells and induce the death of CRL-1623 cells.

3.5. MT changes the expression of lncRNAs in CRL-1623 cells

Epigenetics perform essential roles in tumor cells are vital parts of epigenetic modifications [36]. We screened six lncRNAs to reveal the effect of MT on lncRNA. We analyzed the expression patterns of these lncRNAs in HNSCC using bioinformatics. *MALAT1*, *H19*, *TUG1,* and *PTTG3P* were up-regulated in cancer tissues, and there was a statistical difference in the expression level of *TUG1*. *DICER1-AS1* and *GAS5* were significantly decreased (Fig. 7A). RT-qPCR was performed to analyze whether the expression levels of lncRNAs changed in CRL-1623 cells treated with MT (Fig. 7B). The RT-qPCR results showed that *MALAT1 and H19* lncRNAs were decreased after treatment with MT (0, 0.5, 1, and 2.5 mmol/L), whereas *DICER1-AS1* and *GAS5* were increased. The effect was strongest at 2.5 mmol/L MT. However, the expression levels of *PTTG3P* and *TUG1* did not change. These results suggest that MT may exert anti-tumor effects by regulating *MALAT1*, *DICER1-AS1*, *H19,* and *GAS5*.

3.6. The anti-tumor effects of MT in vivo

CRL-1623 transplantation tumor models were established in nude mice to analyze the inhibitory effect of MT on CRL-1623 *in vivo*.

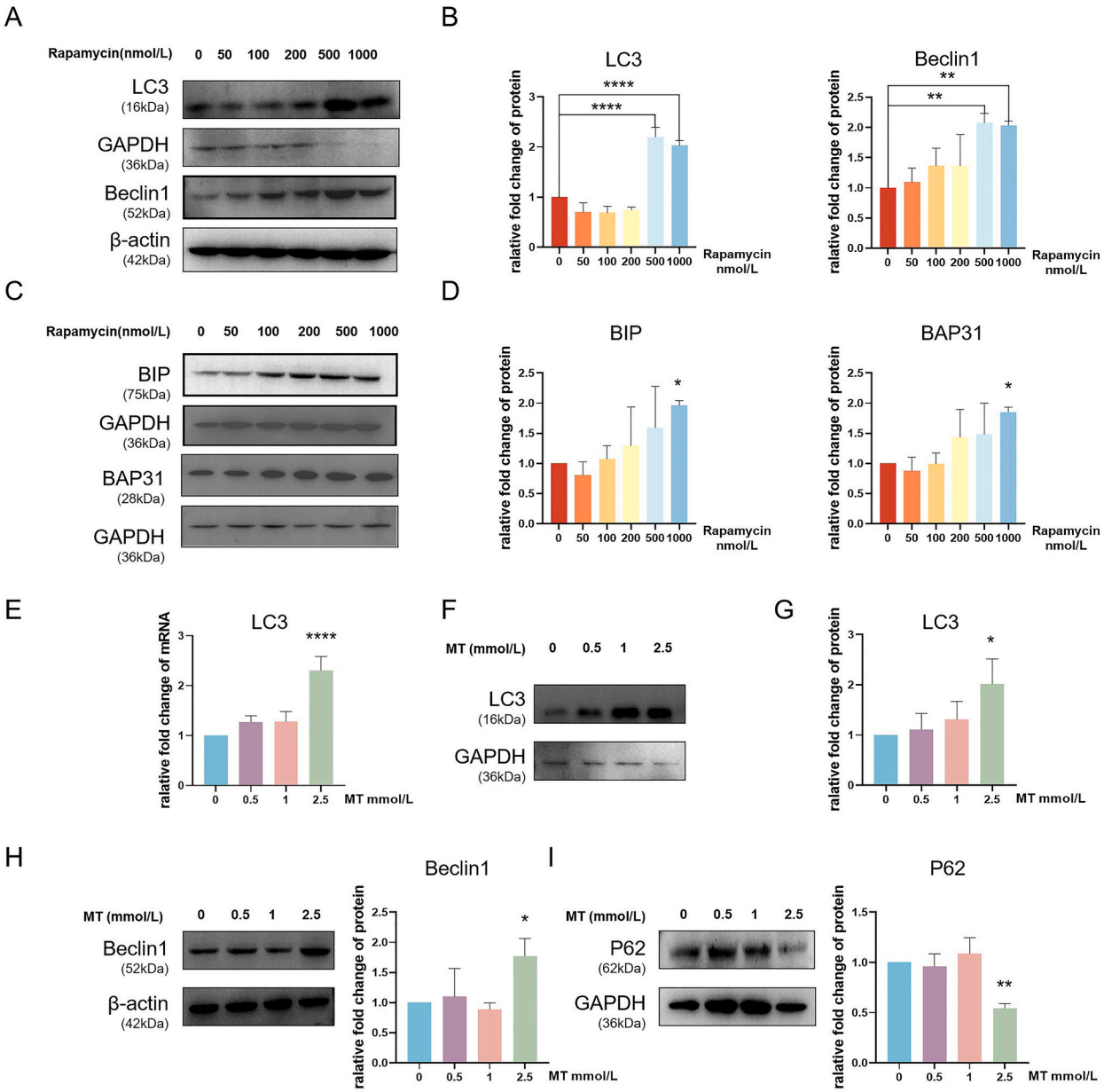

Fig. 5. (A–D) CRL-1623 cells treated with different concentrations of rapamycin were analyzed by Western Blot for LC3, BAP31, Bip and Beclin1 protein expression. Bar graphs illustrate the quantitative analysis of LC3, BAP31, Bip, and Beclin1 proteins. (E–G) RT-qPCR experiment and Western Blot were performed to evaluate the mRNA and protein expression of LC3 after treating CRL-1623 cells with different concentrations of MT. The bar graph shows the quantitative mRNA and protein analysis of LC3. Non-adjusted images for Western blot are included as Supplementary Material. (H–I) The expression of Beclin1 and p62 protein were analyzed by Western Blot after treating CRL-1623 cells with different concentrations of MT, and the bar graphs show the quantitative analysis of Beclin1 and p62. Non-adjusted images for Western blot are included as Supplementary Material. *P < 0.05, **P < 0.01, ****P < 0.0001 vs. 0 mmol/L.

MT was injected intraperitoneally (75 mg/kg/2d) ten days after model establishment when the tumor volume reached 60–100 mm^3 (Fig. 8A). The results show that tumor weight and volume were significantly reduced after MT treatment and suggest that MT could inhibit tumor growth *in vivo* (Fig. 8B–D).

4. Discussion

Chemotherapy is usually used to prolong the survival of patients with advanced TSCC [37]. Nevertheless, resistance to chemotherapy usually appears during treatment and leads to more aggressive tumor behaviors and poor prognosis [37,38]. Chemotherapy

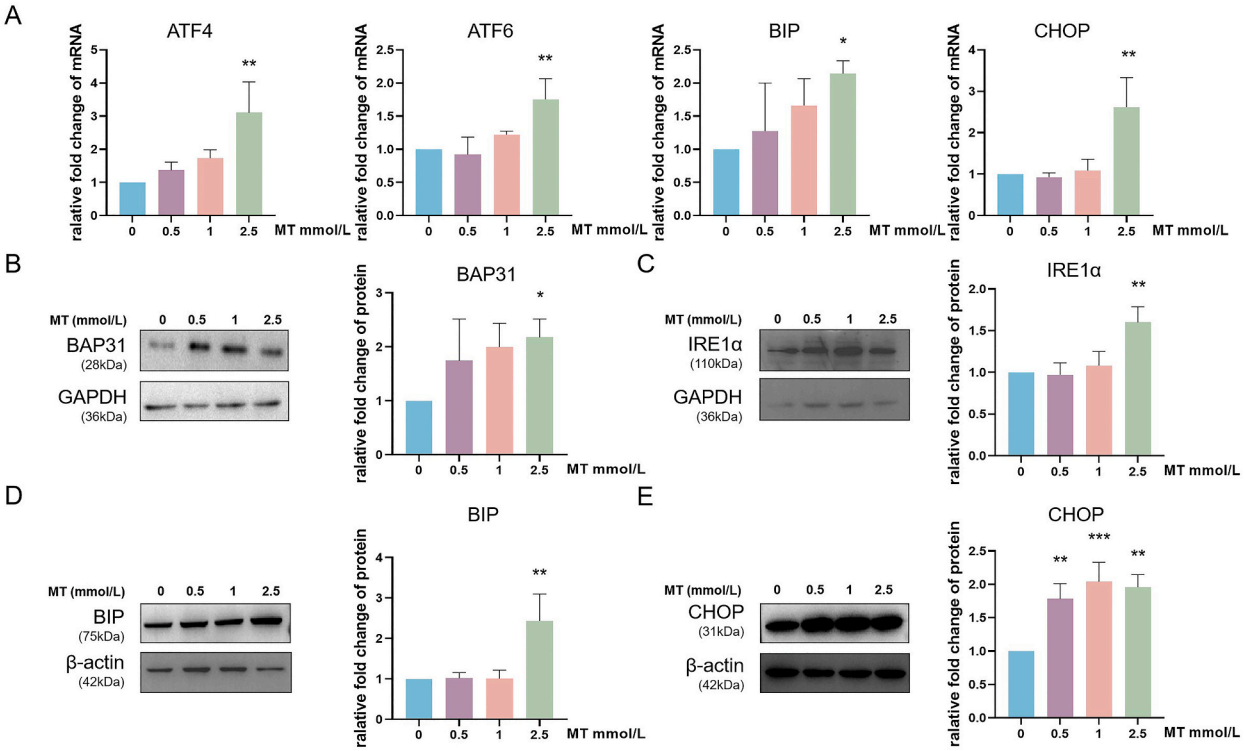

Fig. 6. MT-induced ER stress. (A) RT-qPCR experiments were made to analyze the mRNA expression of ATF4, ATF6, Bip and CHOP after different concentrations of MT treatment in CRL-1623 cells. Bar graphs show the quantitative mRNA analysis of ATF4, ATF6, Bip and CHOP. (B–E) Western Blot was performed to evaluate the expression of BAP31, IER1α, BIP and CHOP after treatment of CRL-1623 cells with different concentrations of MT. Bar graphs show the quantitative analysis of BAP31, IER1α, BIP and CHOP proteins. Non-adjusted images for Western blot are included as Supplementary Material. *P < 0.05, **P < 0.01, ***P < 0.001 vs. 0 mmol/L.

resistance is still one of the major barriers to the clinical treatment of TSCC(38). Therefore, the search for less toxic natural alternatives has become essential. MT is an indole compound shown to play a role in a variety of cancers [7]. Although MT has been associated with excessive sedation, drowsiness, dizziness, nausea, and fatigue in patients [39,40], the combination of MT with chemotherapy drugs or radiotherapy could reduce the side effects of radiotherapy or chemotherapy and improve treatment efficacy [41,42]. MT was previously suggested to promote the mitochondrial function of TSCC cells and enhance their sensitivity to cisplatin and radiation [43,44]. MT was also reported to inhibit folate metabolism and the progression of HNSCC(44). Our study suggested that MT could inhibit cell growth and metastasis and induce autophagy and apoptosis. Thus, the results showed that MT exerted a certain inhibitory effect on CRL-1623 cells (Fig. 9). The previous reports suggested that mice injected with 2 g/kg and 4 g/kg DMSO intraperitoneally did not show any toxic effects [45]. However, toxic effects were observed when the DMSO dose reached 8 g/kg [45]. The MT concentration chosen for our experiments does not produce any toxic effects in mice.

Cell death is critical for maintaining homeostasis [46] and the progression of cancer [47]. One of the characteristics of cancer cells is resistance to death. Apoptosis and autophagic death are the classical forms of cell death [48]. The exogenous death receptor and intrinsic mitochondrial pathways are the core pathways of cell apoptosis [49]. Exogenous pathways are initiated by tumor necrosis factor receptors (TNFRs), Fas (CD95/Apo1), and TNF-associated apoptosis-inducing ligand receptors (TRAILRs), which are death receptors [50]. Intrinsic apoptotic pathways are regulated by proteins in the Bcl-2 family, including pro-apoptotic members (Bax, Bak, Bad, Bcl-Xs, BID, Bik, Bim, HRK, Noxa, and PUMA) and anti-apoptotic members (Bcl-2, Bcl-Xl, Bcl-W, Bcl-1, and MCL-1) [51]. As the results showed, MT promoted HRK, TNFRSF10A, and TNFRSF10B and increased the BAX/BCL-2 ratio. This suggests that MT might induce CRL-1623 cell apoptosis through both the intrinsic mitochondrial pathway and exogenous pathways. Autophagy was initially thought to be a cell survival mechanism [52,53]. However, recent studies suggested that it mediates cell death [52,53]. Autophagy is a catabolic process in cells that aim to degrade and recover cytoplasmic or aggregated proteins and defective organelles [54] and is also a critical process in tumor cells [55]. Beclin1 and LC3 are markers of autophagy, and the p62 protein is the substrate of autophagy. When autophagy is active, the expression of Beclin1 and LC3 is up-regulated, whereas the expression of p62 is decreased [56]. In this study, we found that MT could up-regulate the autophagy-related genes Beclin1 and LC3 and decrease the expression level of p62 protein in CRL-1623 cells, indicating that MT could induce autophagy and trigger cell death in CRL-1623 cells. Furthermore, a previous study demonstrated that PI3K/AKT/mTOR signaling was closely associated with the progression of head and neck squamous cell carcinoma (HNSCC) [57]. The mTOR inhibitor rapamycin targets the mTOR signaling pathway, and MT was found to work by regulating the PI3K/AKT/mTOR signaling pathway to inhibit tumor growth [58]. Therefore, we validated the role of MT with the aid of rapamycin.

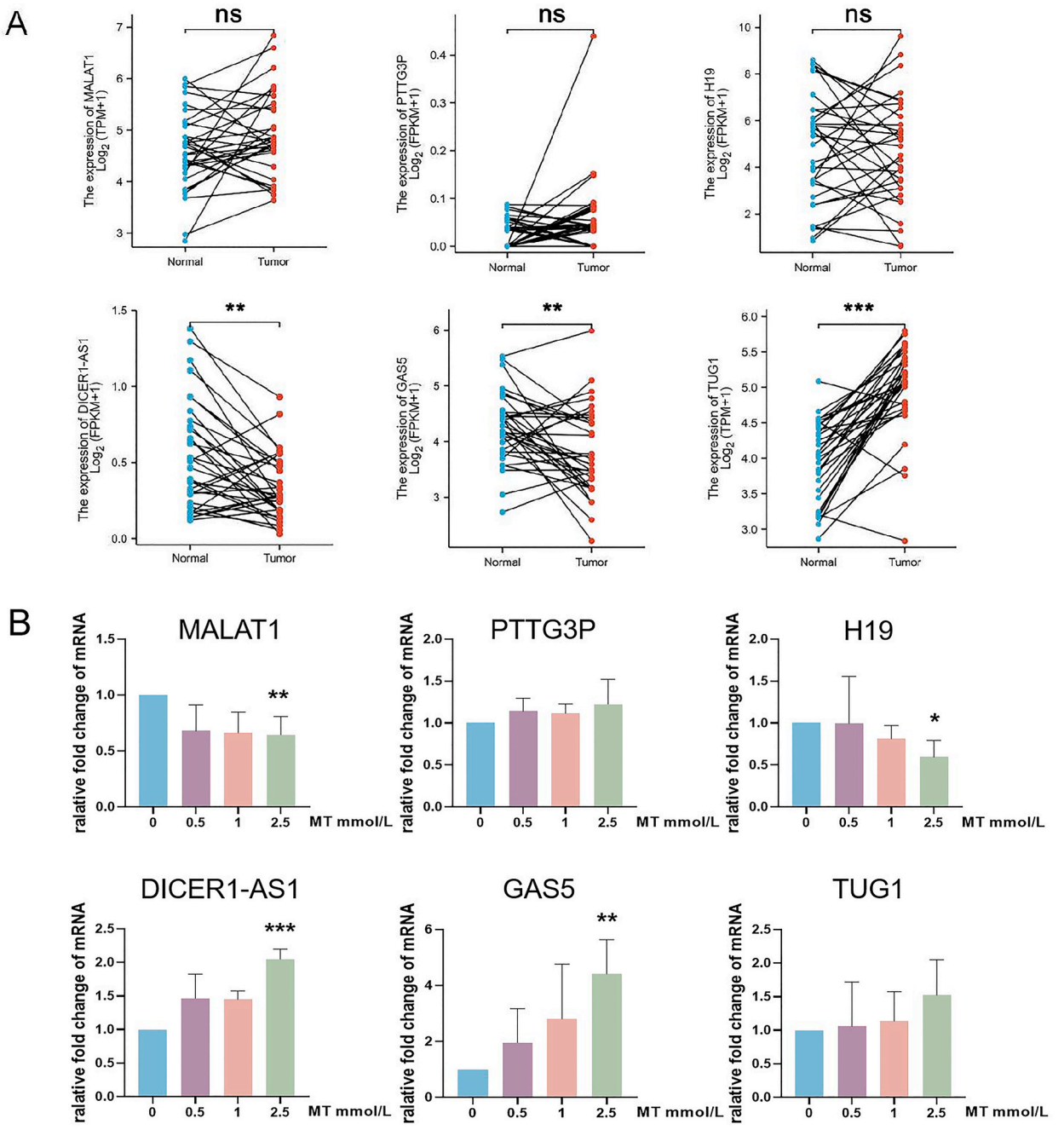

Fig. 7. MT alters the expression levels of LncRNAs in cells. (A) Bioinformatics analysis of LncRNAs in HNSCC. Six LncRNAs were selected to analyze their expression levels in HNSCC by bioinformatics. (B) The expression of the LncRNAs was analyzed by RT-qPCR assay after treating CRL-1623 cells with different concentrations of MT. The bar graph shows the mRNA quantification of the LncRNAs. *P < 0.05, **P < 0.01, ***P < 0.001 vs. 0 mmol/L.

Apoptosis and autophagy are influenced by multiple factors, such as ER stress and epigenetic modification [59–62]. ER is an important organelle in eukaryotic cells and plays critical roles [24] by participating in many biological processes, including protein synthesis and calcium homeostasis [63]. ER is also involved in some other intracellular regulatory pathways, such as autophagy, apoptosis, and inflammation [64]. The unfolded protein response (UPR) is a stress response to protect cells from stimulation, leading to the accumulation of many immature proteins after ER environment damage [64]. ER stress plays a dual role in tumor cells [65,66]. In the short term, the occurrence of UPR helps cancer cells to adapt to the anoxic environment, leading to the rapid growth of tumor cells. However, long-term UPR leads to toxic effects and induces apoptosis [64]. The long-term activation of UPR was reported to induce cell

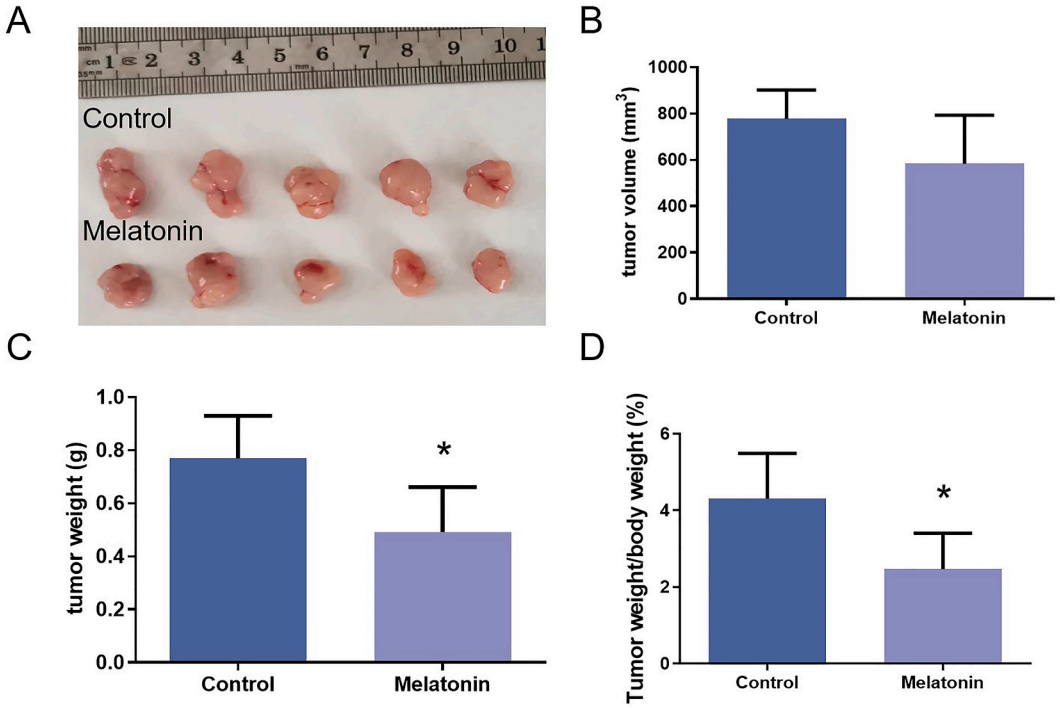

Fig. 8. MT inhibited tumor growth *in vivo*. (A) Morphological observation of TSCC tumor tissues in nude mouse xenograft tumor model (N = 5 in each group). (B) Tumor volume analysis and (C) Tumor weight analysis. (D) The ratio of tumor weight to body weight in nude mice. *P < 0.05 vs. Control.

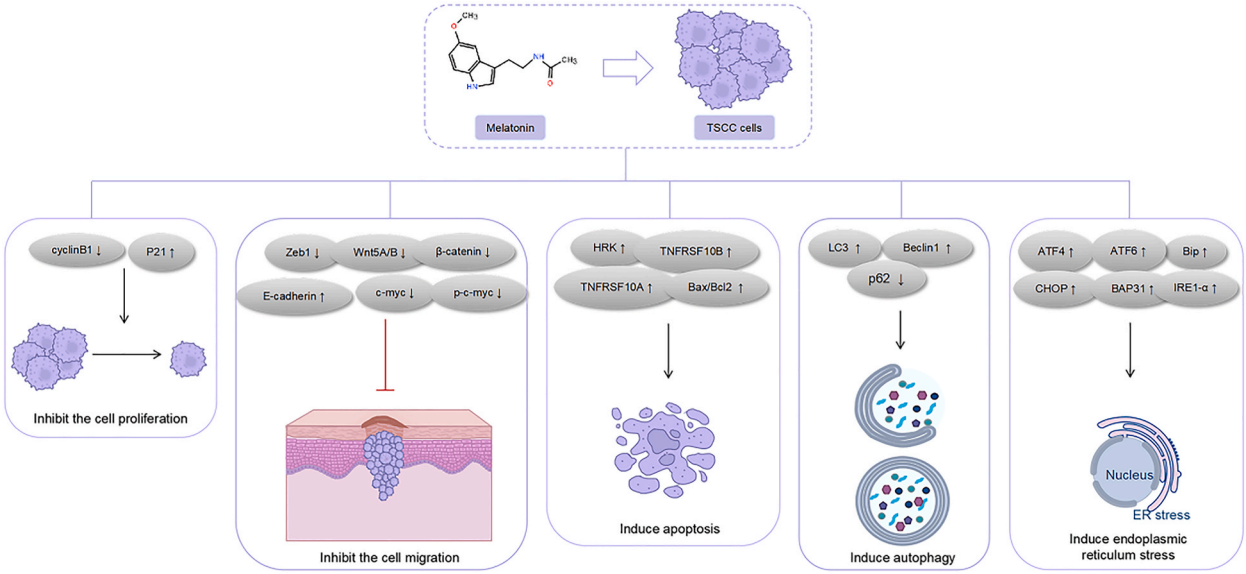

Fig. 9. MT inhibited proliferation and metastasis and promoted apoptosis, autophagy, and endoplasmic reticulum autophagy in TSCC.

apoptosis and autophagy, leading to cell death [54,67]. Our studies showed that MT induced ER stress by up-regulating the expression of ATF4, ATF6, Bip, BAP31, and CHOP and activating the IRE1-α pathway in CRL-1623 cells.

LncRNAs have been proven to function in various cancers [68]. *MALAT1* expression was elevated in oral squamous cell carcinoma (OSCC) and promoted proliferation and metastasis [69]. Knocking down *MALAT1* interfered with intracellular homeostasis, promoted ER stress, induced autophagy and apoptosis, and blocked the cell cycle [69,70].The expression of *H19* was increased in TSCC and facilitated invasion and migration via miR-let-7(70). *TUG1* promoted the invasion and migration of liver cancer cells [71]. *PTTG3P*

promoted invasion, migration, and the proliferation of hepatocellular carcinoma *in vitro* [72]. *DICER1-AS1* expression was decreased in multidrug-resistant osteosarcoma cells and was involved in the mechanism of drug resistance [73]. *GAS5* was expressed at low levels in laryngeal squamous cell carcinoma, and the high expression of *GAS5* promoted autophagy [74]. In our study, the expression of *MALAT1* decreased, while the expression of *GAS5* increased in CRL-1623 cells treated with MT.

In summary, this study successfully unveils the significant anti-cancer properties of MT through *in vitro* experimentation. We investigated the effects of MT on CRL-1623 cells, particularly its ability to stimulate ER stress responses through BAP31, IRE1α, CHOP, and BIP. Additionally, we discovered that MT activates apoptotic and autophagic pathways involving bax, bcl-2, LC3, beclin-1, and p62. MT also upregulated the expression of *DICER1-AS1* and *GAS5*, and downregulated *MALAT1* and *H19*. Combined with preliminary *in vivo* experimental results, our findings lay a foundation for further exploration of MT's potential in the treatment of TSCC. The encouraging outcomes of our study suggest that MT, as a natural compound, holds significant value for further research in the treatment of TSCC.

Data availability statement

Our data will be publicly available through suitable platforms or repositories after a certain period following the acceptance of our research paper. We will ensure the accuracy and completeness of the data and maintain it post-publication. Requests for access to our data can be made through our website or by email. We will provide a timely response and supply the required data access details and instructions.

Ethics approval and consent to participate

The Table of Animal Experimental Ethical Inspection, JLU (permit number: SY202109003).

Patient consent for publication

Not applicable

Funding

This work was supported by Fundamental Research Funds from the Jilin Province Department of Finance (grant no. jcsz2021893-13), Jilin University Youth Faculty-Student Interdisciplinary Project (2022-JCXK-10), the Jilin Province Scientific and Technological Development Program (grant no. 20240305037YY, 20210204013YY, YDZJ202301ZYTS166 and 20220505033ZP), and Beijing Natural Science Foundation (grant no.7244508).

CRediT authorship contribution statement

Huimin Liu: Writing – original draft, Investigation, Formal analysis, Data curation. **Ye Zheng:** Investigation. **Shaoning Kan:** Investigation. **Ming Hao:** Investigation. **Huan Jiang:** Investigation. **Shuangji Li:** Investigation. **Rong Li:** Investigation. **Yinyu Wang:** Investigation. **Dongxu Wang:** Writing – review & editing, Writing – original draft. **Weiwei Liu:** Writing – review & editing, Data curation.

Declaration of competing interest

The authors declare that they have no known competing financial interests or personal relationships that could have appeared to influence the work reported in this paper.

Acknowledgments

Not applicable.

Appendix A. Supplementary data

Supplementary data to this article can be found online at https://doi.org/10.1016/j.heliyon.2024.e29291.

References

[1] B. Solomon, R.J. Young, D. Rischin, Head and neck squamous cell carcinoma: Genomics and emerging biomarkers for immunomodulatory cancer treatments, Semin. Cancer Biol. 52 (2018) 228–240.
[2] A. Jemal, R. Siegel, E. Ward, T. Murray, J. Xu, M.J. Thun, Cancer statistics, 2007, CA Cancer J Clin 57 (2007) 43–66.

[3] B. Tao, D. Wang, S. Yang, et al., Cucurbitacin B inhibits cell proliferation by regulating X-inactive specific transcript expression in tongue cancer, Front. Oncol. 11 (2021) 651648.
[4] Z. Yang, D. Liu, H. Zhou, et al., A new nanomaterial based on extracellular vesicles containing chrysin-induced cell apoptosis through let-7a in tongue squamous cell carcinoma, Front. Bioeng. Biotechnol. 9 (2021) 766380.
[5] B.A. Murphy, S. Ridner, N. Wells, M. Dietrich, Quality of life research in head and neck cancer: a review of the current state of the science, Crit. Rev. Oncol. Hematol. 62 (2007) 251–267.
[6] Y. Xiang, Z. Guo, P. Zhu, J. Chen, Y. Huang, Traditional Chinese medicine as a cancer treatment: modern perspectives of ancient but advanced science, Cancer Med. 8 (2019) 1958–1975.
[7] W.H. Talib, Melatonin and cancer hallmarks, Molecules 23 (2018).
[8] A.T. Slominski, R. Hardeland, M.A. Zmijewski, R.M. Slominski, R.J. Reiter, R. Paus, Melatonin: a cutaneous perspective on its production, metabolism, and functions, J. Invest. Dermatol. 138 (2018) 490–499.
[9] K. Back, D.X. Tan, R.J. Reiter, Melatonin biosynthesis in plants: multiple pathways catalyze tryptophan to melatonin in the cytoplasm or chloroplasts, J. Pineal Res. 61 (2016) 426–437.
[10] N. Zisapel, New perspectives on the role of melatonin in human sleep, circadian rhythms and their regulation, Br. J. Pharmacol. 175 (2018) 3190–3199.
[11] A. Carrillo-Vico, P.J. Lardone, N. Alvarez-Sanchez, A. Rodriguez-Rodriguez, J.M. Guerrero, Melatonin: buffering the immune system, Int. J. Mol. Sci. 14 (2013) 8638–8683.
[12] R. Das, A.A. Balmik, S. Chinnathambi, Melatonin reduces GSK3beta-mediated tau phosphorylation, enhances Nrf2 nuclear translocation and anti-inflammation, ASN Neuro 12 (2020) 1759091420981204.
[13] Z. Fu, Y. Jiao, J. Wang, et al., Cardioprotective role of melatonin in acute myocardial infarction, Front. Physiol. 11 (2020) 366.
[14] L. Xia, C. Sun, H. Zhu, et al., Melatonin protects against thoracic aortic aneurysm and dissection through SIRT1-dependent regulation of oxidative stress and vascular smooth muscle cell loss, J. Pineal Res. 69 (2020) e12661.
[15] E. Nooshinfar, A. Safaroghli-Azar, D. Bashash, M.E. Akbari, Melatonin, an inhibitory agent in breast cancer, Breast Cancer 24 (2017) 42–51.
[16] R.J. Reiter, S.A. Rosales-Corral, D.X. Tan, et al., Melatonin, a full service anti-cancer agent: inhibition of initiation, progression and metastasis, Int. J. Mol. Sci. 18 (2017).
[17] A. Nyamsambuu, M.A. Khan, X. Zhou, H.C. Chen, Molecular mechanism of inhibitory effects of melatonin on prostate cancer cell proliferation, migration and invasion, PLoS One 17 (2022) e0261341.
[18] R. Shafabakhsh, R.J. Reiter, H. Mirzaei, S.N. Teymoordash, Z. Asemi, Melatonin: a new inhibitor agent for cervical cancer treatment, J. Cell. Physiol. 234 (2019) 21670–21682.
[19] K.C. Chok, R.Y. Koh, M.G. Ng, P.Y. Ng, Chye SM: melatonin induces autophagy via reactive oxygen species-mediated endoplasmic reticulum stress pathway in colorectal cancer cells, Molecules 26 (2021).
[20] J. Zhang, J. Guo, N. Yang, Y. Huang, T. Hu, C. Rao, Endoplasmic reticulum stress-mediated cell death in liver injury, Cell Death Dis. 13 (2022) 1051.
[21] X. Fu, J. Cui, X. Meng, et al., Endoplasmic reticulum stress, cell death and tumor: association between endoplasmic reticulum stress and the apoptosis pathway in tumors, Oncol. Rep. 45 (2021) 801–808 (Review).
[22] R. Sitia, I. Braakman, Quality control in the endoplasmic reticulum protein factory, Nature 426 (2003) 891–894.
[23] R.J. Kaufman, Orchestrating the unfolded protein response in health and disease, J. Clin. Invest. 110 (2002) 1389–1398.
[24] C. Hetz, K. Zhang, R.J. Kaufman, Mechanisms, regulation and functions of the unfolded protein response, Nat. Rev. Mol. Cell Biol. 21 (2020) 421–438.
[25] Z. Lin, L. Sun, S. Xie, et al., Chemotherapy-induced long non-coding RNA 1 promotes metastasis and chemo-resistance of TSCC via the wnt/beta-catenin signaling pathway, Mol. Ther. 26 (2018) 1494–1508.
[26] R. Zhao, S. Wang, L. Tan, H. Li, J. Liu, S. Zhang, IGFL2-AS1 facilitates tongue squamous cell carcinoma progression via Wnt/beta-catenin signaling pathway, Oral Dis. 29 (2023) 469–482.
[27] Y. Ren, J. Da, J. Ren, Y. Song, J. Han, An autophagy-related long non-coding RNA signature in tongue squamous cell carcinoma, BMC Oral Health 23 (2023) 120.
[28] Y. Yang, D. Chen, H. Liu, K. Yang, Increased expression of lncRNA CASC9 promotes tumor progression by suppressing autophagy-mediated cell apoptosis via the AKT/mTOR pathway in oral squamous cell carcinoma, Cell Death Dis. 10 (2019) 41.
[29] L. Chang, D. Wang, S. Kan, et al., Ginsenoside Rd inhibits migration and invasion of tongue cancer cells through H19/miR-675-5p/CDH1 axis, J. Appl. Oral Sci. 30 (2022) e20220144.
[30] H.T. Sakurai, H. Iwashita, S. Arakawa, et al., Development of small fluorescent probes for the analysis of autophagy kinetics, iScience 26 (2023) 107218.
[31] B.V. Jardim-Perassi, A.S. Arbab, L.C. Ferreira, et al., Effect of melatonin on tumor growth and angiogenesis in xenograft model of breast cancer, PLoS One 9 (2014) e85311.
[32] E. Jeruzalska, A.J. Mazur, The Role of non-muscle actin paralogs in cell cycle progression and proliferation, Eur. J. Cell Biol. 102 (2023) 151315.
[33] L.R. Pack, L.H. Daigh, T. Meyer, Putting the brakes on the cell cycle: mechanisms of cellular growth arrest, Curr. Opin. Cell Biol. 60 (2019) 106–113.
[34] D. Sano, J.N. Myers, Metastasis of squamous cell carcinoma of the oral tongue, Cancer Metastasis Rev. 26 (2007) 645–662.
[35] C. Kim, B. Kim, Anti-cancer natural products and their bioactive compounds inducing ER stress-mediated apoptosis: a review, Nutrients 10 (2018).
[36] F. Recillas-Targa, Cancer epigenetics: an overview, Arch. Med. Res. 53 (2022) 732–740.
[37] Y. Gu, H. Liu, F. Kong, et al., miR-22/KAT6B axis is a chemotherapeutic determiner via regulation of PI3k-Akt-NF-kB pathway in tongue squamous cell carcinoma, J. Exp. Clin. Cancer Res. 37 (2018) 164.
[38] D.F. Xue, S.T. Pan, G. Huang, J.X. Qiu, ROS enhances the cytotoxicity of cisplatin by inducing apoptosis and autophagy in tongue squamous cell carcinoma cells, Int. J. Biochem. Cell Biol. 122 (2020) 105732.
[39] A.G. Vinther, M.H. Claesson, [The influence of melatonin on the immune system and cancer], Ugeskr Laeger 177 (2015) V10140568.
[40] Thomas CR. Vijayalaxmi Jr., Reiter RJ and Herman TS: melatonin: from basic research to cancer treatment clinics, J. Clin. Oncol. 20 (2002) 2575–2601.
[41] W.H. Talib, A.R. Alsayed, A. Abuawad, S. Daoud, A.I. Mahmod, Melatonin in cancer treatment: current knowledge and future opportunities, Molecules 26 (2021).
[42] B. Jung, N. Ahmad, Melatonin in cancer management: progress and promise, Cancer Res. 66 (2006) 9789–9793.
[43] B.I. Fernandez-Gil, A. Guerra-Librero, Y.Q. Shen, et al., Melatonin enhances cisplatin and radiation cytotoxicity in head and neck squamous cell carcinoma by stimulating mitochondrial ROS generation, apoptosis, and autophagy, Oxid. Med. Cell. Longev. (2019) 7187128.
[44] L. Cui, X. Zhao, Z. Jin, H. Wang, S.F. Yang, S. Hu, Melatonin modulates metabolic remodeling in HNSCC by suppressing MTHFD1L-formate axis, J. Pineal Res. 71 (2021) e12767.
[45] K. Aita, H. Irie, Y. Tanuma, et al., Apoptosis in murine lymphoid organs following intraperitoneal administration of dimethyl sulfoxide (DMSO), Exp. Mol. Pathol. 79 (2005) 265–271.
[46] O. Morana, W. Wood, C.D. Gregory, The apoptosis paradox in cancer, Int. J. Mol. Sci. 23 (2022).
[47] A. Strasser, D.L. Vaux, Cell death in the origin and treatment of cancer, Mol Cell 78 (2020) 1045–1054.
[48] W. Chaabane, S.D. User, M. El-Gazzah, et al., Autophagy, apoptosis, mitoptosis and necrosis: interdependence between those pathways and effects on cancer, Arch. Immunol. Ther. Exp. 61 (2013) 43–58.
[49] A. Ashkenazi, Targeting the extrinsic apoptotic pathway in cancer: lessons learned and future directions, J. Clin. Invest. 125 (2015) 487–489.
[50] G. Liu, F. Pei, F. Yang, et al., Role of autophagy and apoptosis in non-small-cell lung cancer, Int. J. Mol. Sci. 18 (2017).
[51] A.N. Hata, J.A. Engelman, A.C. Faber, The BCL2 family: key mediators of the apoptotic response to targeted anticancer therapeutics, Cancer Discov. 5 (2015) 475–487.
[52] D. Denton, S. Nicolson, S. Kumar, Cell death by autophagy: facts and apparent artefacts, Cell Death Differ. 19 (2012) 87–95.
[53] A.L. Anding, E.H. Baehrecke, Autophagy in cell life and cell death, Curr. Top. Dev. Biol. 114 (2015) 67–91.

[54] T. Yorimitsu, U. Nair, Z. Yang, D.J. Klionsky, Endoplasmic reticulum stress triggers autophagy, J. Biol. Chem. 281 (2006) 30299–30304.
[55] J.M.M. Levy, C.G. Towers, A. Thorburn, Targeting autophagy in cancer, Nat. Rev. Cancer 17 (2017) 528–542.
[56] M. Lippai, P. Low, The role of the selective adaptor p62 and ubiquitin-like proteins in autophagy, BioMed Res. Int. (2014) 832704.
[57] F.E. Marquard, M. Jucker, PI3K/AKT/mTOR signaling as a molecular target in head and neck cancer, Biochem. Pharmacol. 172 (2020) 113729.
[58] K. Chen, P. Zhu, W. Chen, K. Luo, X.J. Shi, W. Zhai, Melatonin inhibits proliferation, migration, and invasion by inducing ROS-mediated apoptosis via suppression of the PI3K/Akt/mTOR signaling pathway in gallbladder cancer cells, Aging (Albany NY) 13 (2021) 22502–22515.
[59] C. Fang, T. Weng, S. Hu, et al., IFN-gamma-induced ER stress impairs autophagy and triggers apoptosis in lung cancer cells, OncoImmunology 10 (2021) 1962591.
[60] Y. Niu, Z. Lin, A. Wan, et al., RNA N6-methyladenosine demethylase FTO promotes breast tumor progression through inhibiting BNIP3, Mol. Cancer 18 (46) (2019).
[61] P. Peixoto, C. Grandvallet, J.P. Feugeas, M. Guittaut, E. Hervouet, Epigenetic control of autophagy in cancer cells: a key process for cancer-related phenotypes, Cells 8 (2019).
[62] M. Bhardwaj, N.M. Leli, C. Koumenis, R.K. Amaravadi, Regulation of autophagy by canonical and non-canonical ER stress responses, Semin. Cancer Biol. 66 (2020) 116–128.
[63] H. Yang, S.H. Park, H.J. Choi, Y. Moon, The integrated stress response-associated signals modulates intestinal tumor cell growth by NSAID-activated gene 1 (NAG-1/MIC-1/PTGF-beta), Carcinogenesis 31 (2010) 703–711.
[64] A. Fernandez, R. Ordonez, R.J. Reiter, J. Gonzalez-Gallego, J.L. Mauriz, Melatonin and endoplasmic reticulum stress: relation to autophagy and apoptosis, J. Pineal Res. 59 (2015) 292–307.
[65] Y.P. Vandewynckel, D. Laukens, A. Geerts, et al., The paradox of the unfolded protein response in cancer, Anticancer Res. 33 (2013) 4683–4694.
[66] Y. Ma, L.M. Hendershot, The role of the unfolded protein response in tumour development: friend or foe? Nat. Rev. Cancer 4 (2004) 966–977.
[67] J.A. Diehl, S.Y. Fuchs, C. Koumenis, The cell biology of the unfolded protein response, Gastroenterology 141 (38–41) (2011) 41 e31–e32.
[68] Y.T. Tan, J.F. Lin, T. Li, J.J. Li, R.H. Xu, H.Q. Ju, LncRNA-mediated posttranslational modifications and reprogramming of energy metabolism in cancer, Cancer Commun. 41 (2021) 109–120.
[69] X. Zhou, S. Liu, G. Cai, et al., Long non coding RNA MALAT1 promotes tumor growth and metastasis by inducing epithelial-mesenchymal transition in oral squamous cell carcinoma, Sci. Rep. 5 (2015) 15972.
[70] N. Kou, S. Liu, X. Li, et al., H19 facilitates tongue squamous cell carcinoma migration and invasion via sponging miR-let-7, Oncol. Res. 27 (2019) 173–182.
[71] L. Lu, J. Huang, J. Mo, et al., Exosomal lncRNA TUG1 from cancer-associated fibroblasts promotes liver cancer cell migration, invasion, and glycolysis by regulating the miR-524-5p/SIX1 axis, Cell. Mol. Biol. Lett. 27 (17) (2022).
[72] J.L. Huang, S.W. Cao, Q.S. Ou, et al., The long non-coding RNA PTTG3P promotes cell growth and metastasis via up-regulating PTTG1 and activating PI3K/AKT signaling in hepatocellular carcinoma, Mol. Cancer 17 (93) (2018).
[73] F. Wang, L. Kong, Y. Pu, et al., Long noncoding RNA DICER1-AS1 functions in methylation regulation on the multi-drugresistance of osteosarcoma cells via miR-34a-5p and GADD45A, Front. Oncol. 11 (2021) 685881.
[74] J. Wang, Y. Zhu, S. Ni, S. Liu, LncRNA GAS5 suppressed proliferation and promoted apoptosis in laryngeal squamous cell carcinoma by targeting MiR-26a-5p and modifying ULK2, Cancer Manag. Res. 13 (2021) 871–887.